

Towards a User Adaptive Assistive Robot: Learning from Demonstration Using Navigation Functions

Xanthi S. Papageorgiou¹, Athanasios C. Dometios², Costas S. Tzafestas²

¹Embodied Interaction and Robotics Group, ILSP, ATHENA RC, Athens Greece

²School of Electrical and Computer Engineering, National Technical University of Athens, Greece

xpapag@athenarc.gr, athdom@mail.ntua.gr, ktzaf@cs.ntua.gr

Abstract—Elderly and mobility impaired people need special attention during bathing activities, since these tasks are demanding in body flexibility. Our aim is to build an assistive robotic bathing system, in order to increase the independence and safety of this procedure. Towards this end, the expertise of professional carers for bathing sequences and appropriate motions have to be adopted, in order to achieve natural, physical human - robot interaction. In this paper a Navigation Function (NF) approach is proposed in order to reproduce the way an expert clinical carer executes the bathing activities by means of construction repulsive potential fields (“virtual obstacles”) for an assistive bath robot. The produced vector field, constructed based on the demonstration procedure, is used for real-time motion behavior planning tasks, which exploits the visual information from Depth sensors and the advantages of the NF approach, to estimate the reference pose for the end-effector of the assistive robotic system. The proposed method guarantees globally asymptotic convergence to the learned from demonstration washing motion, within the deformable and moving body-part limits, while in addition, restricted areas on the body surface are avoided. The proposed method is evaluated using real experimental data, obtained from human subjects during pouring water task demonstration.

I. INTRODUCTION

Activities of Daily Living, especially body care (bathing or showering), dressing, eating, etc., are demanding procedures in terms of effort and body flexibility, [1], [2]. Elderly people, who have special and increased needs for attention during those activities (clinical and in-house) will induce great financial and social onus to the insurance systems and also to their families. Robotic solutions have already been recently proposed to help disabled and elderly people with special needs, in these personal care activities. Most of them focus on a specific body part, [3], or support people on performing other personal care activities with rigid manipulators, [4].

Showering activities are highly demanding tasks in terms of safety, since they are imposing direct physical contact between the human and the assistive device. In case of an assistive robotic system, the execution of the tasks should handle successfully further constraints prescribed by the fact

This research work has received funding from the EU’s Horizon 2020 research and innovation programme under grant agreement No 643666:“I-SUPPORT” and by the European Union and Greek national funds through the Operational Program Competitiveness, Entrepreneurship and Innovation, under the call RESEARCH – CREATE – INNOVATE (i-Walk project code:T1EDK- 01248 / MIS: 5030856, <http://www.i-walk.gr/>).

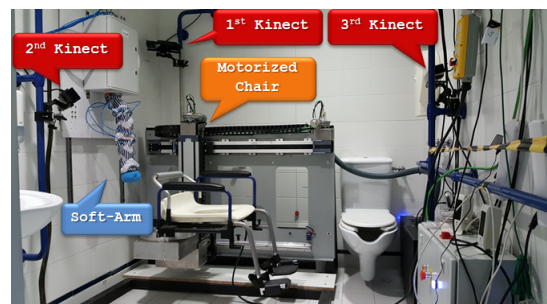


Fig. 1: The real experimental robotic bath system in a pilot study. that the robot has to operate on curved, deformable human body parts within dynamic environments, since non predictable body-part’s motion may occur during the execution of the tasks. Natural and effective human - robot physical interaction is a key characteristic from system safety and from user acceptance point of view. Planning of human-friendly washing actions in terms of motion and force exertion on each body part is inherently difficult. Thus, proper washing motions should be learned from demonstration of clinical experts, in order to incorporate their skills into the system.

Skill learning from demonstration has been thoroughly addressed in previous approaches [5]. Several generic models and representations have been proposed in this context, such as HMM [6] and GMM [7]. More recent approaches, use dynamical systems [8], [9] in the form of Dynamic Movement Primitives (DMP), which incorporate a spring damping system to encode attractive behaviours to primitive actions, whose variety is captured by a coupling force term. On the other hand, in [10], the inverse problem of estimating a repulsive field of unknown obstacles from knowledge of feasible trajectories was investigated with application to grasping based on a NF methodology. In this approach the authors propose a gradient descent method to construct an obstacle space, which, when navigated using a NF based approach, produces trajectories similar to the learned trajectories. This method can be used on trajectories that can be produced by a limited set of obstacles, i.e. when a suitable convex target function can be constructed, for the optimization scheme.

Washing action learning is an interactive task, which combines the execution of a complex motion relatively to the body part. Robotic interactive behaviour learning has also been based on motion primitives as presented in [11]–[13]. In [14]

a DMP a leader-follower framework has been developed, which takes the environment’s motion into consideration. However, planning robotic actions with DMPs does not consider the presence of obstacles in the workspace. In previous works [15]–[17] the authors combined DMP approach with Dynamic Potential Fields in order to achieve obstacle avoidance. However, the appearance of local minima can trap the agent before reaching its destination. Navigation Functions (NF) have been proposed to overcome the local minima problem, [18], [19]. In our previous work based on a NF approach, [20], [21] we have proposed a vision based motion planning framework, which achieve the adaptation of motion primitives on moving, deformable surfaces, with simultaneous obstacle avoidance. To this end, the robotic system has to incorporate a suitable sensing subsystem. The recent advances of computer vision algorithms with Deep Learning approaches have presented promising results on human perception and body-part’s segmentation, [22]–[24].

In this paper a NF approach is proposed in order to capture the way an expert clinical carer executes the bathing activities by means of construction “virtual obstacles”. The bathing trajectories demonstration is realized in 3D space and are transformed to a 2D spatially normalized space by establishing appropriate transformations. In this space, a set of virtual obstacles is calculated so that the trajectory produced by a NF resembles the human trajectories, in effect, the human trajectory is represented in the virtual obstacles. Also, we propose an extension of our previous planning framework, [20], in order to smoothly integrate our learning method into the bathing system. The proposed method is evaluated through real experiments in two different showering scenarios. The demonstration trajectories were visually captured by using a Kinect camera and a more complex obtained from the publicly available KIT whole-body human motion database [25], in order to demonstrate the applicability of the proposed approach on real body parts.

II. PROBLEM STATEMENT

The motion behavior problem of a robotic manipulator’s end-effector, which operates over a curved, deformable surface (e.g. user’s body part), in a workspace equipped with a depth-camera, is considered. Following [20] the control problem is reduced to an equivalent problem in the 2D Canonical space. Using this transformation, we shall use this 2D space for our control and learning schemes. In that space, we assume that the robot can be kinematically described by $\dot{\mathbf{q}} = \mathbf{u}$, where \mathbf{q} is the vector of end-effector position and orientation, and \mathbf{u} is the vector of velocity inputs. Let the admissible and feasible state space (workspace) for the robot be denoted $\mathcal{W} \subset \mathbb{R}^2$. The obstacle free subset of \mathcal{W} is denoted $\mathcal{W}_{free} \subseteq \mathcal{W}$. Also, we define a NF $\varphi : \mathcal{W} \rightarrow \mathbb{R}$ which models the environment, and with \mathbf{q}_d is the NF’s target configuration. Let $\mathcal{O} \subseteq \mathcal{W} \setminus \mathcal{W}_{free}$ be the set of all obstacles in \mathcal{W} . These obstacles correspond to real obstacle in the task space that are visible by a depth camera, whose field of view should include the workspace of the robot and may regard

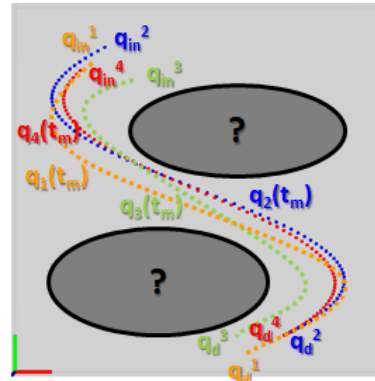


Fig. 2: Problem Statement: Find the obstacle functions based on the collected experimental human like trajectories $\mathbf{q}(t_m)$, to ensure that the new controller-based produced motion will always remain within the problem’s domain.

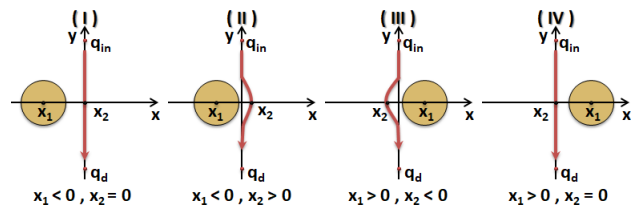


Fig. 3: Point robot motion planning problem on a 2D workspace that contains one cyclic obstacle.

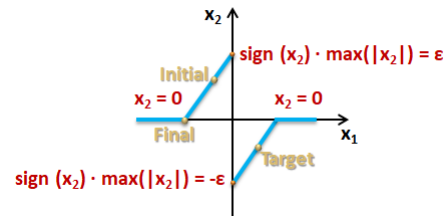


Fig. 4: The relation between the the obstacle’s center on x_1 -axis and the distance of the resulted path from the y -axis x_2 .

restricted areas, on the user’s body (e.g. local injuries), which should be avoided during the washing sequence.

We utilize a NF which is at least C^2 , admissible (uniformly maximal on the boundary), Morse (non-degenerate critical points) and Polar (unique global minimum at \mathbf{q}_d), as:

$$\varphi(\mathbf{q}, t) = \frac{\gamma(\mathbf{q}, t)}{[\gamma^\kappa(\mathbf{q}, t) + \beta(\mathbf{q}, t)]^{1/\kappa}} \quad (1)$$

where $\kappa > 0$, $\gamma \triangleq \|\mathbf{q} - \mathbf{q}_d\|^2$ is the distance to the goal function (attractive potential field), and $\beta(\mathbf{q}) \triangleq \prod_{i=0}^P \beta_i$, $\forall i = 0, 1, \dots, P$ is the product of P obstacle functions, where for $i = 0$ is the workspace boundary obstacle, coming from visual feedback (repulsive potential field), [19].

The robotic shower system in Fig. 1, aims to support elderly or people with mobility disabilities during showering activities, i.e. pouring water, soaping, body part scrubbing, etc. Assume that we have a set of $T_{exp} \in \mathbb{N}^* \triangleq \mathbb{N} \setminus \{0\}$ demonstrated trajectories by nursing experts, E_n , $n \in N_{exp} \triangleq \{1, 2, \dots, T_{exp}\}$. Each of them is a set $E_n \triangleq \{\mathbf{q}_n(t_m)\}_{m \in N_n}$, $N_n \triangleq \{1, 2, \dots, T_n\}$, $n \in N_{exp}$ of $T_n \in \mathbb{N}^*$ configurations $\mathbf{q}_n(t_m) \in \mathcal{W} \subset \mathbb{R}^2$ recorded in subsequent time instants

$t_m \in [0, +\infty)$, which are indexed in increasing order $t_m < t_{m+1}$, $\forall m \in N_n \setminus \{T_n\}$, $\forall n \in N_{exp}$. Assume that the desired destinations $\mathbf{q}_{dn} \in \mathcal{W}$, $n \in N_{exp}$ are provided. The problem is summarized in developing a motion planning framework, which incorporates a proper learning strategy to learn human-friendly washing actions from demonstration of experts and adapts the learned motions to the user's body parts.

III. PROPOSED APPROACH

A learning strategy is proposed separately for the periodic and the discrete actions. For the latter, which constitute the main part of the motion, the proposed solution is to produce a suitable vector field, the motion under which replicates the demonstrated data. This approach is clearly advantageous, as the incorporation of the learned data in a vector field allows their immediate combination with real time obstacles detected by the system. The problem can be stated as in Fig. 2. We intent to use the experimental data $E \triangleq \{E_n, \mathbf{q}_{dn}\}_{N_{exp}}$ in order to find the obstacle function $\beta \in C^2(E^n, \mathbb{R})$, so that the produced trajectory from the following controller:

$$\dot{\mathbf{q}} = -\nabla_{\mathbf{q}}\varphi(\mathbf{q}) \quad (2)$$

is similar to the experimental trajectories, defined by an appropriate similarity measure. Since it is not a simple path similarity problem, we propose to use the Fréchet distance [26], as the distance metric between two trajectories in the state space. This is a measure of similarity between two curves, that takes into account the flow of two curves, because the pairs of points whose distance contributes to the distance sweep continuously along their respective curves. This metric is defined as the maximum distance between two agents moving forward on the two trajectories and actively trying to keep their distance to a minimum and it is more "naturally" way of estimating the distance of two curves, in a setting such as ours. In layman terms, the output of the controller should approximate the experimental trajectories.

Consequently, we need a measure on how much two given trajectories "resemble" each other. One distance measure possibility consists in approximating each curve by a set of points and then using the Hausdorff distance. However, the Hausdorff distance only takes into account the sets of points on both curves and does not reflect the course of the curves.

The Fréchet distance can be illustrated as: suppose a man is walking his dog and that he is constrained to walk on a curve and his dog on another curve. Both the man and the dog are allowed to control their speed independently, but are not allowed to go backwards. Then, the Fréchet distance of the curves is the minimal length of a leash that is necessary.

Definition 1: Let S a metric space. A curve $A \in S$ is a continuous map from the unit interval into S , i.e. $A : [0, 1] \rightarrow S$. A reparameterization α is a continuous, non-decreasing, surjection $\alpha : [0, 1] \rightarrow [0, 1]$. Let A and Λ be two given curves in S . Then, the Fréchet distance between A and Λ is defined as the infimum over all reparameterizations $\alpha, \lambda \in [0, 1]$ of the maximum over all $t \in [0, 1]$ of the distance in S between $A(\alpha(t))$ and $\Lambda(\lambda(t))$. The Fréchet distance F is defined as:

$$F(A, \Lambda) = \inf_{\alpha, \lambda} \max_{t \in [0, 1]} \{d(A(\alpha(t)), \Lambda(\lambda(t)))\} \quad (3)$$

where d is the distance function of S . \square

This measure takes the value 0 when the trajectories are equal and grows positively as the curves become more dissimilar.

A. Obstacle Function Resolution Formulation

The main goal is to formulate an appropriate equation, the resolution of which will produce the unknown obstacle function β (the repulsive field). The proposed problem formulation guarantees that the produced potential field, based on the constructed NF, models the carer's motions during the washing tasks. In other words, this approach creates the learning by demonstration procedure of washing models.

Let the NF of (1), and we can take it's derivative: $\nabla_{\mathbf{q}}\varphi(\mathbf{q}, \mathbf{q}_d) = \frac{\partial\varphi}{\partial\gamma}(\gamma, \beta) \cdot \nabla_{\mathbf{q}}\gamma(\mathbf{q}, \mathbf{q}_d) + \frac{\partial\varphi}{\partial\beta}(\gamma, \beta) \cdot \nabla_{\mathbf{q}}\beta(\mathbf{q})$. Therefore, it holds that: $\frac{\partial\varphi}{\partial\gamma} = \beta \cdot A$, $\frac{\partial\varphi}{\partial\beta} = -\frac{\gamma}{\kappa} \cdot A$, $\nabla\gamma = 2 \cdot (\mathbf{q} - \mathbf{q}_d)$, where $A = (\gamma^\kappa + \beta)^{-\left(\frac{\kappa+1}{\kappa}\right)}$. Also, based on the obstacle function definition: $\nabla\beta = \beta \cdot \sum_{i=0}^P \frac{\nabla\beta_i}{\beta_i}$. In this work, we form an obstacle function structure β_i , for $i = 1, \dots, Q$, with $Q < P$, where P is the total number of obstacles, for simplicity as ellipsoid function and thus, the main goal is to compute the necessary parameters in order to construct these "virtual obstacles", i.e. centers and length of the principal axes.

In [10], the solution is based on a gradient descent method, that produces the obstacle function. Moreover, the authors use the gradient of the experimental trajectories in order to compute the cost function to be optimized. This resolution is feasible for convex case studies, otherwise the gradient descent method maybe trapped in local minima.

B. Non-Convexity of the Inverse Problem

When \mathcal{W} contains obstacles in its interior, the NF becomes highly entangled w.r.t. the position and obstacles' general form. Due to this aspect, the estimation of the appropriate set of parameters for the obstacles that generated a NF with the desired form equates into solving a problem that is non convex. The proof of this statement is presented next.

Assume the problem of a point robot motion planning on a 2D workspace. Let for simplicity, the initial and desired configurations of the robot lies on the y-axis, anti-symmetrically of the x-axis. The optimum path to resolve this motion planning problem is for the robot to follow a path that lies on the y-axis (following the line $x = 0$). As one simple cyclic obstacle appears in the workspace, the motion planning resolution of this case depends on the relative position of the obstacle. Assuming that x_1 is the obstacle's center on x-axis and x_2 is the distance of the resulted path from the y-axis, we can distinguish four general cases for the obstacles relative position w.r.t y-axis, as described in Fig. 3. As the obstacle is away from the y-axis there are two cases, when the obstacle region is in negative side of y-axis (**I**), and when it is in the positive side of y-axis (**IV**), Fig. 3. In these cases the resulted optimal path remain on the y-axis and therefore the distance $x_2 = 0$. In the other two cases of Fig. 3, it holds that for case (**II**) the distance $x_2 > 0$, while for case (**III**) it switches $x_2 < 0$. Thus, the relation between

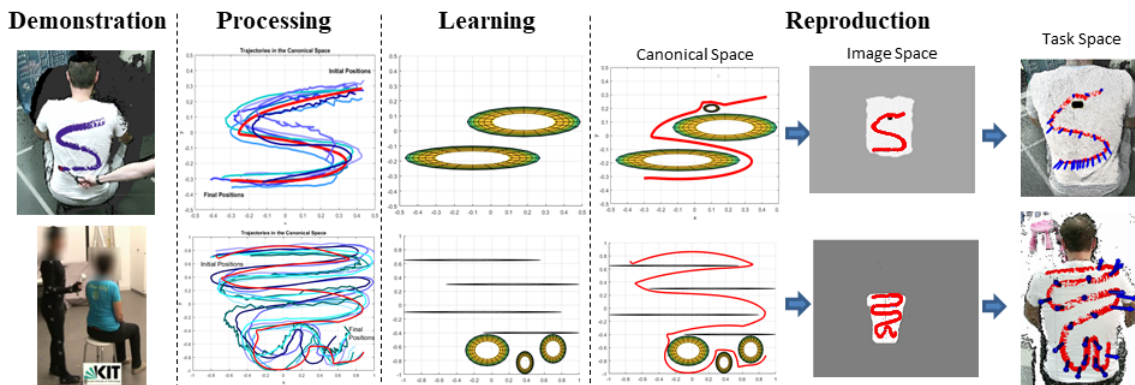


Fig. 5: The **Demonstration** trajectories are performed in physical space by professional nursing personnel. The demonstration data are projected into the $2D$ canonical space, in which are post-**Processed**. In the **Learning** phase virtual obstacles are learned using the demonstration data and the proposed NF approach. During the trajectory **Reproduction** phase a NF controller is employed to reproduce the washing action. The learned trajectory (red) is then adapted on the visually segmented back region (PointCloud view) of a subject, via the image space. **Top**: A simple showering sinusoidal trajectory is visually recorded, learned and reproduced. **Bottom**: A more complex showering trajectory is obtained from the KIT whole-body human motion database [25], learned and reproduced.

x_1 and x_2 is described in Fig. 4. This figure demonstrates the highly non-convex character of the optimization problem. On that figure, a point on the left side of the diagram (with negative x_2 deflection) cannot move, using gradient descent to the right side of the diagram (positive x_2 deflection). If the initial position of the obstacle is point **Initial**, Fig. 4, a gradient descent will push away the obstacle towards point **Final**, i.e. will push the obstacle further away to the left. It is not possible for a gradient descent method to converge to point **Target**, i.e. an obstacle to the right of the y -axis. A gradient descent algorithm will result in the obstacle being “pushed away”. Therefore there is no way to resolve this problem with a simple gradient descent method.

C. Non-Convex Inverse Problem Resolution

The recorded experimental data are usually very noisy, as it can be realized from the second column of Fig. 5. A numerical differentiation scheme would result in excessive noise added to the system. Thus, we propose to resolve the optimization problem in the entire recorded trajectory, by using the Fréchet distance metric (*Definition 1*).

Another important issue is that the problem is highly non-convex, as it is described in the previous subsection. The optimization procedure, in order to resolve the inverse problem, that is based on a simple gradient descent method cannot result to a feasible solution and requires the use of some kind of heuristic approaches. Thus, we used a Genetic Algorithm (GA) solution as the form of the problem is naturally suited for such an approach. In particular, the parameters of the obstacles are naturally suited genes for a GA, since, to an extent, the positions of the obstacle, the size and its form have a differential effect on the form of the NF trajectory and to the cost of the optimization function.

In order to augment the GA search, a gradient descent method [27] is used, as local optimization scheme for every member of each generation, as: $x^{(j+1)} = x^{(j)} - \omega \cdot \nabla C$, minimizing the cost function C , where x^j denotes the obstacle parameter values at the j^{th} iteration of minimization procedure and ω is the design space cost functional gradient

step. Obviously, this augmentation will have the detrimental effect described above for some sets of solutions (will drive the obstacles away from the correct positions).

Then, it is necessary to formulate the optimization cost function C for the discrete samples, as following: $C \triangleq \frac{1}{T_{exp}} \cdot \sum_{n \in N_{exp}} F(R, E_n)$, where F is the Fréchet distance defined by (3), E_n is an experimentally measured trajectory, while R is the estimated trajectory composed by the candidate obstacle function β . Each estimated point $(\mu + 1)$ of the trajectory R is computed based on the previous point (μ) by the equation: $\mathbf{q}^{(\mu+1)} = \mathbf{q}^{(\mu)} + \Delta t \cdot \dot{\mathbf{q}}$, where Δt is the time step between the points and $\dot{\mathbf{q}}$ is calculated as in (2). The C code for the Discrete Fréchet implementation was adopted from [28]. The GA [29] was adopted and programmed in C/C++ from [30].

IV. PERCEPTION-BASED ROBOT BEHAVIOR ADAPTATION USING DEPTH SENSOR DATA

The main task of the proposed approach is to learn by demonstration appropriate washing actions e.g. pouring water. The demonstration is performed in the physical space, hence a post-processing procedure followed in which the demonstration examples were projected in a $2D$ spatially normalized space denoted as canonical space, following the notation of our previous work [20]. In this simplified space the demonstration paths are denoised and the discrete part is separated from any periodic motion, as in the second column of Fig. 5. In this form the demonstration data are used in the learning procedure described in Section III, in which a set of virtual obstacles is generated forming a repulsive landscape, which encodes the demonstrated washing skill.

The “virtual obstacle” function β is then used in the reproduction phase. At this stage an initial and goal configuration is provided to the system and fed into the following controller to generate a washing action, which satisfies the constraints imposed by the health-care specialist and the constraints imposed by the region of action. For brevity, we only present the definition of the behavioral based motion controller.

Proposition 1: The system $\dot{\mathbf{q}} = \mathbf{u}$ under the control law $\mathbf{u} = -\nabla_{\mathbf{q}} \varphi(\mathbf{q}(t))$, with φ as defined in (1) is globally

asymptotically stable, almost everywhere. Proof in [31].

Based on this motion controller the next desired position is extracted in the $2D$ canonical space and propagated to the $3D$ task space for execution from the assistive robotic device. More specifically, each generated point is projected using anisotropic scaling and proper rotation into the $2D$ image space. On this space, image segmentation techniques (either simple cartesian and color filters or more sophisticated approaches [22]–[24]) can be applied, which provide a detailed image mask containing only the corresponding to the body-part pixels. From this output mask, we are able to calculate the center and the extends of the body-part area and hence to associate each path point to these geometric characteristics. Then, the point from the image space is projected, through the camera projection transformation, in order for the robot to be able to navigate on any point of the surface that needs to be washed (e.g. the back of the user). It is able to locally calculate the geometric attributes of the body-part’s surface, from the Depth data captured by the camera, as described in [20], in order to provide the proper reference pose to a robotic manipulator, that will execute the washing task. The described transformations can also work as a feedback to the controller. In case of obstacle area detection in the task space (e.g. injuries on the body part, represented by the black area in the top right part of Fig. 5), the aforementioned transformations project them to the canonical space, in order to incorporate them to the NF controller. The learned from demonstration behaviour could be modified in a way that the restricted areas of the body part to be avoided, as shown in the top of Reproduction phase of Fig. 5.

V. EXPERIMENTS

A. Setup Description

In order to test and analyze the performance of the proposed approach, an experimental setup is used that includes a Kinect-v2 Camera providing depth data for the back region of a subject. For the demonstration procedure simple sinusoidal trajectories were visually captured by the camera. The carer holds a marker and he/she performs a pouring water like motion on the specific body part. The subject is seated and he/she is free to move their back as he/she wants (twist, slight turn, etc.). The only constraint is to remain seated during the recordings and to avoid extreme movements, in order to keep the body part region inside the camera’s field of view, top of Fig. 5. A more complex demonstration example obtained from the publicly available KIT whole-body human motion database [25], as in bottom of Fig. 5. Thus, during this validation study the main goal is to imitate the way that the expert clinical carer executes the task. Therefore, our goal is to reproduce this execution no matter how effective the carer’s motion is or how complex and comprehensive this activity is (e.g. coverage percentage).

B. Validation Strategy and Results

The experimental data consists of trajectory data from demonstration by professional clinical carers for pouring

water sequence in the $3D$ task space that have been transformed for learning purposes in the $2D$ canonical space. These trajectories in the canonical space are depicted with blue scaled colours in Fig. 5 (second column).

After the proposed learning from the demonstration data approach in the canonical space (i.e. the “virtual” obstacles have been incorporated), the NF controller estimates the feasible, optimal trajectory in the canonical space, by providing to it, just the initial and destination position and by taking into account the users body structure and restrictions (i.e. the real obstacles that have been recognized in the task space and they have been also transformed to the canonical space). The evaluation procedure imposes the decision of random initial and destination positions in the canonical space.

For testing purposes we decide to use the recorded data in order to compare the NF-based produced trajectory w.r.t. the carer’s demonstration in the canonical space. In Fig. 6, both trajectories are plotted. The red lines represent the controller-based trajectory while with the blue lines are the demonstrated washing task execution. The discrete Fréchet distances is zero when the two trajectories are equal and grows positively as the curves become more dissimilar. Based on these results, these trajectories are very similar (based on the Fréchet distance metric), since this metric take values 0.052 and 0.198, respectively. Another qualitative conclude is that the resulted trajectories are very smooth, highly appropriate for execution by any assistive robotic device.

In Fig. 5 (Reproduction), a learned trajectory is adapted on a $3D$ deformable back region of a subject, which is visually perceived by the camera (PointCloud view). The estimated local perpendicular vectors (blue) are also demonstrated in several segments of the executed path. Based on them, the ability of the proposed approach to apply any learned trajectory in the canonical space to any $3D$ subject’s body part surface with unknown curvature, motion and deformation is demonstrated. In Fig. 5 (top), a learned trajectory is adapted on a $3D$ deformable male’s subject back region, which is visually perceived by the camera, and also compensates a real obstacle (e.g. a restricted area) of a subject’s body part.

VI. CONCLUSIONS AND FUTURE WORK

This paper presents an efficient NF approach for learning from demonstration the behavior of an expert clinical carer during the execution of bathing activities by means of constructing repulsive potential fields (“virtual obstacles”). The constructed vector field, based on the learning procedure, is used for real-time motion behavior planning tasks, which exploits the visual information from Depth sensors, in order to calculate the reference position for the end-effector of the assistive robotic system, whose task is to interact in a friendly way with moving and variably curved body parts.

The proposed method is validated through real carer’s demonstration recorded data. The experimental results show, that the planning system is able to learn the expert’s skills by producing similar paths (based on the Fréchet distance metric) with the respective demonstrated trajectories, providing very smooth, highly appropriate for execution by any

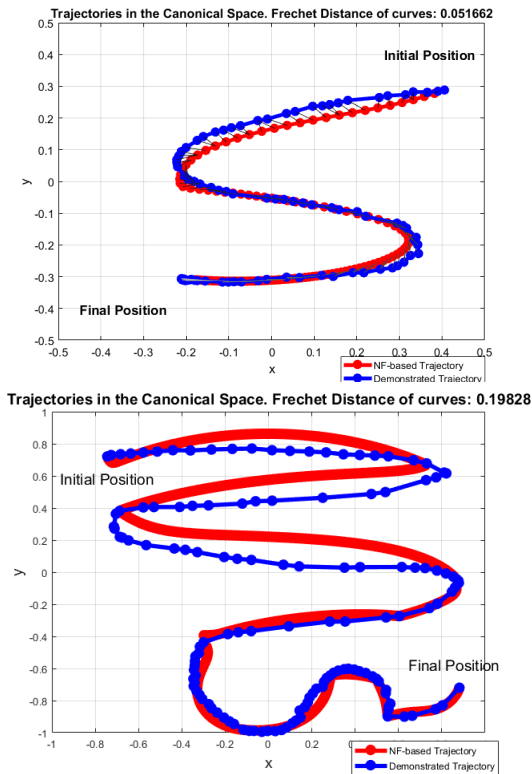


Fig. 6: Comparison of the NF-based produced trajectory w.r.t. the carer's demonstration in the canonical space.

assistive robotic devices carer's-like paths. This approach is very suitable for adapting the variable subject's preferences w.r.t. to time and way of washing tasks execution.

An explicit comparison between our work and a DMP based approach is not straightforward, as it requires a complex DMP to incorporate all the constraints of our problem and the quality of the DMP implementation is a key element to the quality of the results. Despite the fact that, in our previous work [21] we have shown smooth integration of our planning framework with DMPs, we are working on an DMP approach for comparison purposes in the learning procedure.

Also, for further research, we aim to improve this methodology for efficient encoding of periodic actions. Since the latter are inherently attractive actions, a different learning strategy has to be adopted. In the learning procedure the GA in essence simply "decides" if the trajectory passes right or left from an obstacle. We plan to use an iterative algorithm which uses a branch procedure and computes all such possible obstacle trajectory combinations, effectively augmenting the GA. In the current version, the number of the obstacles is set by the user, while a GA approach could use an open number of obstacles, the efficacy of such a procedure would be low. An approach in which the number of obstacles is estimated by an algorithm would be beneficial.

REFERENCES

[1] D. D. Dunlop and et.al., "Disability in activities of daily living: patterns of change and a hierarchy of disability," *American Journal of Public Health*, pp. 378–383, 1997.
 [2] S. Katz and et.al., "Studies of illness in the aged: The index of adl: a standardized measure of biological and psychosocial function," *JAMA*, pp. 914–919, 1963.

[3] T. Hirose and et.al., "Development of hair-washing robot equipped with scrubbing fingers," in *ICRA*, 2012.
 [4] M. Hillman and et.al., "The weston wheelchair mounted assistive robot - the design story," *Robotica*, vol. 20, pp. 125–132, 3 2002.
 [5] B. D. Argall and et.al., "A survey of robot learning from demonstration," *Robot. Auton. Syst.*, 2009.
 [6] D. Kulić, Takano, and et.al., "Incremental learning, clustering and hierarchy formation of whole body motion patterns using adaptive hidden markov chains," *The International Journal of Robotics Research*, 2008.
 [7] S. Calinon and et.al., "On learning, representing, and generalizing a task in a humanoid robot," *IEEE Transactions on Systems, Man, and Cybernetics, Part B*, 2007.
 [8] A. J. Ijspeert and et.al., "Dynamical movement primitives: learning attractor models for motor behaviors," *Neural computation*, vol. 25, no. 2, pp. 328–373, 2013.
 [9] S. Schaal, "Dynamic movement primitives-a framework for motor control in humans and humanoid robotics," in *Adaptive Motion of Animals and Machines*. Springer, 2006, pp. 261–280.
 [10] I. F. Filippidis, K. J. Kyriakopoulos, and P. K. Artemiadis, "Navigation functions learning from experiments: Application to anthropomorphic grasping," in *2012 IEEE International Conference on Robotics and Automation*, May 2012, pp. 570–575.
 [11] M. Mühlig, M. Gienger, and J. J. Steil, "Interactive imitation learning of object movement skills," *Autonomous Robots*, pp. 97–114, 2012.
 [12] T. Kulvicius, M. Biehl, M. J. Aein, M. Tamosiunaite, and F. Wörgötter, "Interaction learning for dynamic movement primitives used in cooperative robotic tasks," *Robotics and Autonomous Systems*, 2013.
 [13] H. B. Amor and et.al., "Interaction primitives for human-robot co-operation tasks," in *IEEE international conference on robotics and automation*, 2014.
 [14] Y. Zhou, M. Do, and T. Asfour, "Coordinate change dynamic movement primitives—a leader-follower approach," in *2016 IEEE/RSJ International Conference on Intelligent Robots and Systems*, 2016.
 [15] D.-H. Park and et.al., "Movement reproduction and obstacle avoidance with dynamic movement primitives and potential fields," in *Humanoids 8th IEEE-RAS International Conference on Humanoid Robots*, 2008.
 [16] P. Pastor and et.al., "Learning and generalization of motor skills by learning from demonstration," in *IEEE ICRA*, 2009.
 [17] M. Chi, Y. Yao, Y. Liu, and M. Zhong, "Learning, generalization, and obstacle avoidance with dynamic movement primitives and dynamic potential fields," *Applied Sciences*, vol. 9, no. 8, p. 1535, 2019.
 [18] D. E. Koditschek and E. Rimon, "Robot navigation functions on manifolds with boundary," *Advances in Applied Mathematics*, 1990.
 [19] E. Rimon and D. Koditschek, "Exact robot navigation using artificial potential functions," *Transactions on Robotics and Automation*, 1992.
 [20] A. C. Dometios, X. S. Papageorgiou, A. Arvanitakis, C. S. Tzafestas, and P. Maragos, "Real-time end-effector motion behavior planning approach using on-line point-cloud data towards a user adaptive assistive bath robot," in *IEEE/RSJ IROS*, 2017.
 [21] A. C. Dometios, Y. Zhou, X. S. Papageorgiou, C. S. Tzafestas, and T. Asfour, "Vision-based online adaptation of motion primitives to dynamic surfaces: application to an interactive robotic wiping task," *IEEE Robotics and Automation Letters*, pp. 1410–1417, 2018.
 [22] L.-C. Chen, G. Papandreou, I. Kokkinos, K. Murphy, and A. L. Yuille, "DeepLab: Semantic image segmentation with deep convolutional nets, atrous convolution, and fully connected crfs," *arXiv:1606.00915*, 2016.
 [23] L.-C. Chen, Y. Yang, J. Wang, W. Xu, and A. L. Yuille, "Attention to scale: Scale-aware semantic image segmentation," in *The IEEE Conference on Computer Vision and Pattern Recognition*, June 2016.
 [24] S.-E. Wei, V. Ramakrishna, T. Kanade, and Y. Sheikh, "Convolutional pose machines," in *IEEE Conference CVPR*, 2016.
 [25] C. Mandery and et.al., "Unifying representations and large-scale whole-body motion databases for studying human motion," *IEEE Transactions on Robotics*, 2016.
 [26] T. Eiter and H. Mannila, "Computing discrete fréchet distance," 1994.
 [27] L. Hasdorff, "Gradient optimization and nonlinear control," 1976.
 [28] M. Pak, "Fast c implementation of the discrete fréchet distance computation for matlab mex."
 [29] Z. Michalewicz, *Genetic Algorithms + Data Structures = Evolution Programs*, 3rd ed. Springer, 1996.
 [30] J. Burkardt, "A simple genetic algorithm," Available at [https://people.sc.fsu.edu/~jburkardt/cpp_src/simple_ga/simple_ga.html\(15/9/2017\)](https://people.sc.fsu.edu/~jburkardt/cpp_src/simple_ga/simple_ga.html(15/9/2017)).
 [31] X. Papageorgiou, S. Loizou, and K. Kyriakopoulos, "Motion planning and trajectory tracking on 2-D manifolds embedded in 3-D workspaces," *2005 IEEE ICRA*, 2005.